Noname manuscript No.
(will be inserted by the editor)

Effects of Tunable Excitation in Carotenoids Explained by the Vibrational Energy Relaxation Approach

Vytautas Balevičius Jr. · **Craig N. Lincoln** · **Daniele Viola** · **Giulio Cerullo** · **Jürgen Hauer** · **Darius Abramavicius**

Received: date / Accepted: date

Abstract Carotenoids are fundamental building blocks of natural light harvesters with convoluted and ultrafast energy deactivation networks. In order to disentangle such complex relaxation dynamics, several studies focused on transient absorption measurements and their dependence on the pump wavelength. However, such findings are inconclusive and sometimes contradictory. In this study, we compare internal conversion dynamics in β-carotene, pumped at the first, second and third vibronic progression peak. Instead of employing data fitting algorithms based on global analysis of the transient absorption spectra, we apply a fully quantum mechanical model to treat the high-frequency symmetric carbon-carbon (C=C and C–C) stretching modes explicitly. This model successfully describes observed population dynamics as well as spectral line shapes in their time-dependence and allows us to reach two conclusions: Firstly, the broadening of the induced absorption upon excess excitation is an effect of vibrational cooling in the first excited state (S_1). Secondly, the internal conversion rate between the second excited state (S_2) and S_1 crucially depends on the relative curve displacement. The latter point serves as a new perspective on solvent- and excitation wavelength dependent experiments and lifts contradictions between several studies found in literature.

Darius Abramavicius
Department of Theoretical Physics, Vilnius University, Sauletekio al. 9-III, 10222 Vilnius, Lithuania
E-mail: darius.abramavicius@ff.vu.lt

Vytautas Balevičius Jr.
School of Biological and Chemical Sciences, Queen Mary University of London, Mile End Road, London E1 4NS, UK

Craig N. Lincoln, Jürgen Hauer
Photonics Institute, TU Wien, Gusshausstr. 27, 1040 Vienna, Austria

Daniele Viola, Giulio Cerullo
IFN-CNR, Dipartimento di Fisica, Politecnico di Milano, Piazza Leonardo da Vinci 32, 20133 Milan, Italy

Keywords internal conversion · β-carotene · transient absorption spectroscopy · vibrational cooling

Introduction

Carotenoids are ubiquitous natural pigment molecules found in plants, bacteria and algae (Young and Britton, 1993; Frank et al, 1999; van Amerongen et al, 2000). They perform a number of functions ranging from light-harvesting in the green-blue spectral region to photoprotection by quenching (bacterio-)chlorophyll triplet states or singlet oxygen (Frank and Cogdell, 1996; Polívka and Sundström, 2004). Despite the huge diversity of this pigment class, the majority of carotenoids are characterized by several common properties. They absorb light into their second excited singlet state S_2, because the first excited singlet state S_1 is optically inaccessible due to symmetry reasons (Polívka and Sundström, 2004). S_2 decays into S_1 with a time constant of $\sim 100-200$ fs, while S_1 further relaxes to the ground state on a time scale from several to tens of picoseconds. This picture is consistent with most of the experimental findings, however, some evidence including quantum chemical calculations suggests involvement of additional optically dark states (Polívka and Sundström, 2009).

In order to understand the intricate photophysics of carotenoids, transient absorption (TA) spectroscopy has been performed systematically on samples of various chain lengths, in different solvents, at different excitation wavelengths, temperature and combinations of these parameters (Larsen et al, 2003; Jailaubekov et al, 2011; Staleva et al, 2015; Takaya and Iwata, 2014). Each of these series provide valuable information.

Excitation energy dependence of carotenoid relaxation dynamics is one of the unsolved problems, which has been studied previously in several works (Nakamura et al, 2004;

Billsten et al, 2005; Kosumi et al, 2005; Nakamura et al, 2006; Zuo et al, 2007; Jailaubekov et al, 2011; Staleva et al, 2015). The attempts to determine the general dependence of S_2 lifetime on excess excitation energy failed to yield an unambiguous answer. All possible trends can be found in literature, from speed-up (Billsten et al, 2005; Zuo et al, 2007) and slow-down of relaxation (Kosumi et al, 2005; Kloz et al, 2012) to no change at all (Staleva et al, 2015).

In this paper we focus on the overall relaxation dynamics of β-carotene as a function of the initially excited vibronic levels on S_2, both theoretically and experimentally. We use a model called Vibrational Energy Relaxation Approach (VERA), which considers four electronic singlet states, S_0, S_1, S_2 and S_n, and treats two high-frequency carbon–carbon stretching modes (single and double bond) explicitly, while the other vibrations are included as a bath (Balevičius Jr. et al, 2015). We previously demonstrated that the inclusion of vibrational levels on states S_1, S_2 and S_n can adequately describe the TA spectra of β-carotene and its artificial derivative. By adding vibrational substructure to the electronic ground state, VERA readily explains the S^* feature found in TA spectra (Balevičius Jr. et al, 2016). In both cases a number of parameters had to be determined by fitting the modeled spectra to the experiment. Some of those parameters can be verified by or determined from other experiments, e.g., the line-shape of ground state bleach (GSB) is obtained from the linear absorption, and the frequencies of the stretching modes are known from the Raman spectra. The crucial parameters determining the internal conversion dynamics between S_2 and S_1 are the energy gap between the states, the displacements between the harmonic oscillators representing the two vibrational modes, and the spectral density of the bath. While the latter cannot be measured directly, e.g., (Wendling et al, 2000), the energy gap and the displacements can be obtained simultaneously from a single experiment, namely TA in the near-infrared (NIR) region covering the S_1 to S_2 transition energy (Polívka et al, 2001; Polívka and Sundström, 2004). While we have used literature-based values for these parameters in our earlier reports, in this study we extract them from experimental TA NIR spectra of β-carotene in two solvents, fixing the maximally consistent set of model parameters. Explicit modeling of internal conversion allows us to explain the seemingly inconsistent results from pump wavelength dependent studies found in literature, both in TA and fluorescence excitation experiments. We show that curve displacement between S_2 and S_1 is a crucial parameter for the internal conversion between the two states. Using VERA, we explain the pump wavelength dependence of this ultrafast population transfer process ($S_2 \rightarrow S_1$) without the need to invoke optically dark intermediate states (Polívka and Sundström, 2009).

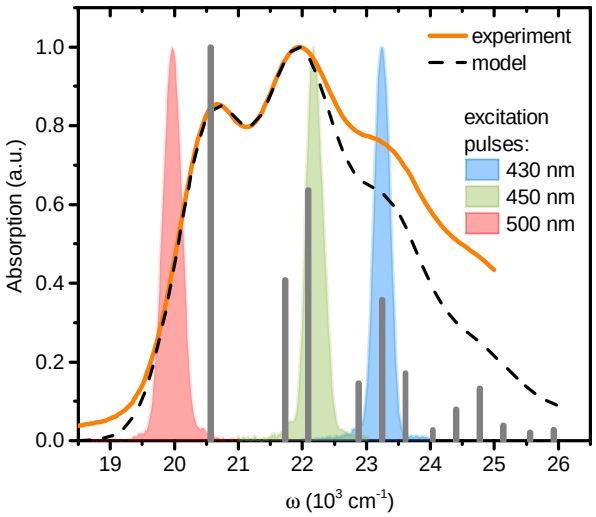

Fig. 1 Absorption spectrum of β-carotene in cyclohexane. Full line shows the experimental data, dashed line corresponds to model calculations. The underlying stick spectrum is shown, where the intensities correspond to the Franck–Condon factors of the specific mode combinations (see text for details). The excitation pulses used in the experiment are also shown at 20000 cm^{-1}, 22200 cm^{-1} and 23250 cm^{-1} (corresponding to 500 nm, 450 nm and 430 nm respectively)

Model and methods

Vibrational energy relaxation approach

Our previously proposed scheme for calculating TA spectra of carotenoids, VERA, is given in detail in (Balevičius Jr. et al, 2015). Essentially, the TA spectrum is shaped by four electronic states coupled to two vibrational modes. The spectrum consists of three components: induced absorption (IA), stimulated emission (SE) and GSB. The IA component is described as the following sum of products:

$$A_{\text{ind.}}(\omega,t) = \sum_i I_i^{ab}(\omega) n_i^{ab}(t). \tag{1}$$

Here $n_i^{ab}(t)$ is the population of the i'th vibronic state, $|i_{ab}\rangle$, and $I_i^{ab}(\omega)$ denotes the sum of spectral profiles associated with the relevant optical transitions originating *from* the i'th state (*vide infra*). The vibronic state $|i_{ab}\rangle$ is defined as the direct product of an electronic and two corresponding vibrational wave-vectors: $|i_{ab}\rangle = |S_i\rangle|a\rangle_1|b\rangle_2$. Here, $|S_i\rangle$ denotes one of the three electronic states, S_0, S_1 and S_2 from which the absorption can take place, and the indices a/b denote the numbers of quanta in the C=C / C–C stretching modes with frequencies $\omega_1 = 1522$ cm^{-1} and $\omega_2 = 1156$ cm^{-1}, respectively.

In this paper, the sums over indices, $\sum_i$, implicitly include the summation over these vibrational indices a or b, with the exception of the electronic ground state, where only

one vibronic level $|0_{00}\rangle$ is considered. (In (Balevičius Jr. et al, 2016) this restriction is lifted.) This is justified, given the focus of the current work on $S_2 \to S_1$ relaxation. Hence we don't include the implicit summation for $i = 0$ in Eq. 1, neglecting the induced absorption from vibrationally hot ground state levels. We have demonstrated that the inclusion of such terms enables the description of the S^* signal in carotenoids longer than β-carotene studied here (Balevičius Jr. et al, 2016).

The spectral shape term, $I_i^{ab}(\omega)$, has the following structure:

$$I_i^{ab}(\omega) = \sum_{j>i} f_{ij}(a,b,a',b')\sigma(\omega - \omega_{ij} - \omega_{a,b,a',b'}, \Delta\omega_{ij}). \quad (2)$$

Here, $\sigma(\omega, \Delta\omega)$ determines the line-shape of an individual optical transition $i \to j$ (either Gaussian or Lorentzian of FWHM $\Delta\omega$), ω_{ij} denotes the purely electronic energy gap (the 0–0 transition), while $\omega_{a,b,a',b'} = \omega_1(a'-a) + \omega_2(b'-b)$ denotes the energy gap ($\hbar = 1$) between the vibrational sub-levels of the electronic states i (indices a, b) and j (primed indices a', b'). The function $f_{ij}(a,b,a',b')$ describes the amplitude of the transition and reads:

$$f_{ij}(a,b,a',b') = |\mu_{ij}|^2 \langle a|a'\rangle_1^2 \langle b|b'\rangle_2^2, \quad (3)$$

where, μ_{ij} is the electronic transition dipole moment of the $i \to j$ transition, and $\langle a|a'\rangle_1$, $\langle b|b'\rangle_2$ are the Franck–Condon (FC) factors describing the overlap between the vibrational wave-functions. The FC factors are determined by the dimensionless displacements, d_1^{ij} and d_2^{ij}, between the potential energy surfaces of the two stretching modes (May and Kühn, 2004).

As for the other optical processes, using the above definitions we recognize that the absorption spectrum is given by $I_0^{00}(\omega)$ and GSB merely flips its sign. Since the only strongly emitting state in carotenoids is S_2, SE can be represented by the term

$$E(\omega,t) = \widetilde{I}_2^{ab}(\omega) n_2^{ab}(t), \quad (4)$$

where the tilde means that $\widetilde{I}_2^{ab}(\omega)$ is given by Eq. 2 with the exception that now $j < i$ (transition to lower lying vibronic levels) and $\omega_{ij} \to \omega_{ij} - \delta\omega_{\mathrm{St.}}$, where $\delta\omega_{\mathrm{St.}}$ is the Stokes shift. Effectively this means that the emission from the lowest lying vibronic level on S_2 is the mirror image of the absorption spectrum $I_0^{00}(\omega)$, red-shifted by the Stokes shift.

Finally the TA spectrum, which is essentially a difference spectrum, is calculated as:

$$\Delta A(\omega,t) = A_{\mathrm{ind.}}(\omega,t) - E(\omega,t) - I_0^{00}(\omega). \quad (5)$$

Alternatively, rearranging the terms we obtain

$$\Delta A(\omega,t) = \sum_{i\neq 0} I_i^{ab}(\omega) n_i^{ab}(t) - E(\omega,t) - I_0^{00}(\omega) \sum_{i\neq 0} n_i^{ab}(t).$$

In the following we refer to the terms on the right hand side as IA, SE and GSB, accordingly.

Population relaxation is governed by a master equation, which is explicitly presented in the Supplementary Information of (Balevičius Jr. et al, 2015). In short, we start from a Hamiltonian comprising two blocks of vibronic levels $|1_{ab}\rangle$ and $|2_{ab}\rangle$. The radiationless decay is caused by the bath-induced off-diagonal fluctuations (Valkunas et al, 2013), where the bath is defined as solvent phonons plus all the remaining vibrational modes of the carotenoid. The fluctuations are described by the correlation functions of the bath. Based on this Hamiltonian, equations of motion are derived within the secular and Markov approximations.

For the initial condition describing the excitation of the carotenoid we include temporal and spectral properties of the pump pulse via a pumping term, $p_{ab}(t)$, in the equations of motion:

$$\frac{\mathrm{d}}{\mathrm{d}t} n_2^{ab}(t)\bigg|_{\mathrm{pump}} = p_{ab}(t,\omega_{\mathrm{p}}), \quad (6)$$

where ω_{p} is the center frequency of the chosen pump pulse, and the (normalized) pumping term itself reads:

$$p_{ab}(t,\omega) = \Gamma(t,\tau_{\mathrm{p}}) f_{02}(0,0,a,b)\sigma(\omega - \omega_{02} - \omega_{0,0,a,b}, \Delta\omega_{\mathrm{p}}); \quad (7)$$

Here, both the temporal and spectral parts, $\Gamma(t,\tau_{\mathrm{p}})$ and $\sigma(\omega, \Delta\omega_{\mathrm{p}})$, are Gaussians of widths τ_{p} and $\Delta\omega_{\mathrm{p}}$, accordingly. The invoked approximations imply that the possible coherent effects (Dobryakov et al, 2005; Christensson et al, 2010) are neglected and the calculated TA at times $t \leq \tau_{\mathrm{p}}$ should be treated with caution.

Transient absorption measurements in NIR and VIS

The ultrafast TA spectroscopy setup is driven by an amplified Ti:sapphire laser (Coherent Libra) giving 4 mJ, 100 fs pulses at 800 nm central wavelength and 1 kHz repetition rate. A part of the pulse energy is used to drive a non-collinear optical parametric amplifier (NOPA) (Cerullo and Silvestri, 2003) to produce the pump pulses, while the probe pulses are generated through tight focusing of a small fraction of the 800 nm laser output into a 3 mm thick CaF_2 plate, producing a white light continuum from 350 to 750 nm for probing in the visible. For probing in the NIR, the CaF_2 plate was replaced by a 6 mm thick YAG plate, yielding a probe spectrum spanning from 860 to 1400 nm. In order to be able

Table 1 Model parameters used in fitting the line-shapes.

transition	solvent	$\omega_{ij}\,(\mathrm{cm}^{-1})$	d_1^{ij}	d_2^{ij}	$\Delta\omega_{ij}, \mathrm{cm}^{-1}$
$S_0 \to S_2$	cyclo.	20570	0.83	0.75	755
$S_1 \to S_n$	cyclo.	17850	0.38	0.39	730
$S_1 \to S_2$	cyclo.	6810	0.78	0.64	400†
$S_0 \to S_2$	tolu.	19830	0.84	0.73	770
$S_1 \to S_2$	tolu.	6550	0.8	0.71	430†

†All the optical line-shapes were fitted using Gaussian profiles; Lorentzian profiles produced better fits for NIR data

to continuously change the pump wavelength from 430 to 490 nm, the NOPA was tuned to the NIR, with pulses between 860 to 980 nm, and its output was frequency-doubled with a β-barium borate crystal. The pump pulse duration, measured by autocorrelation, was approximately 70 fs. After the sample, the probe spectra were recorded by a spectrometer, triggered at the laser repetition rate and capable of single-shot detection. The pump pulse is modulated by a chopper at half the laser repetition rate. Transmitted probe spectra are recorded in the presence (T_{ON}) and in the absence (T_{OFF}) of the pump. These spectra are processed in order to get the differential transmission signal as $\Delta T/T = (T_{\mathrm{ON}} - T_{\mathrm{OFF}})/T_{\mathrm{OFF}}$ at every pump–probe delay. For sample preparation, β-carotene (Sigma-Aldrich) was dissolved in either cyclohexane or toluene (HPLC-grade), to yield solutions of less than 0.4 OD maximum absorption in the visible. Absorption as well as TA measurements were carried out in a quartz cuvette with 1 mm light path length.

Results

Absorption spectra and induced absorption in the NIR

The absorption spectrum of β-carotene in cyclohexane is shown in Fig. 1. This is a typical absorption spectrum of carotenoids expressing a well-resolved progression of vibronic peaks (Polívka and Sundström, 2004). The spectrum in toluene (not shown) is qualitatively very similar, except for a red-shift discussed below.

An absorption experiment determines the parameters describing the line-shape of the $S_0 \to S_2$ transition. Because for carotenoids $\mu_{01} = 0.0$ we only need to fit $\omega_{02}, d_1^{02}, d_2^{02}$ and $\Delta\omega_{02}$ (we chose $\mu_{02} = 1.0$ in arbitrary units for scaling). The calculated absorption spectrum $I_0^{00}(\omega)$ is plotted by the dashed line in Fig. 1; Gaussian line-shapes were used. The parameters determining the optical transitions are given in Table 1, along with the parameters for the spectrum in toluene for comparison. The most notable difference is the 740 cm^{-1} red-shift with respect to the absorption maximum in cyclohexane.

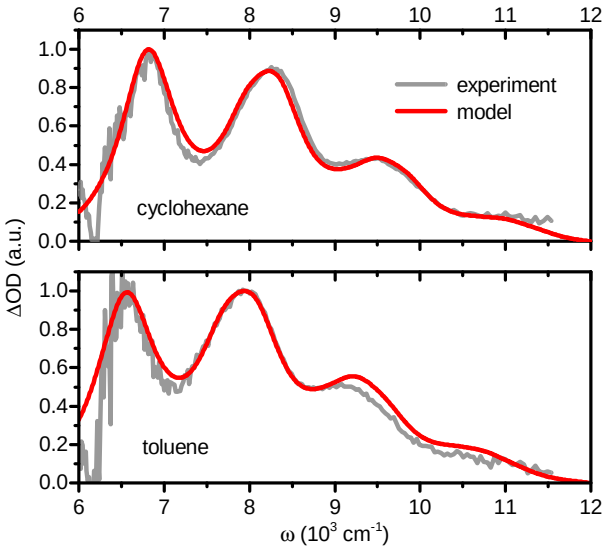

Fig. 2 NIR transient absorption spectra 2 ps after 500 nm excitation. Experimental data are shown as fuzzy lines. Results in cyclohexane and toluene are depicted in top and bottom panels, accordingly. Model calculations are represented by smooth lines

As can be seen, the model accurately describes the first two peaks, 0–0 and 0–1, but fails at higher frequencies, where the experimental intensity is larger. It was argued previously that the high energy spectrum of carotenoids might be influenced by a distribution of geometrical conformers (Lukeš et al, 2011; Papagiannakis et al, 2006; Hauer et al, 2013; Chábera et al, 2009), which would not be captured by our model.

The gray stick spectrum shows the values of the function $f_{02}(0,0,a,b)$, conf. Eq. 3, at the corresponding wavenumbers $\omega_{02} + \omega_{0,0,a,b}$, normalized to the value $f_{02}(0,0,0,0)$ (first peak in the series). The stick spectrum is useful for illustrating how the selective excitation is achieved. For example, the 500 nm pulse is only in resonance with the 0–0 peak, whereas the pulses of shorter wavelength cover several levels within the vibrational progression.

NIR TA spectra for β-carotene in cyclohexane and toluene after 500 nm excitation are shown in Fig. 2. The spectra are recorded at 2 ps delay, thus after relaxation from S_2 to S_1. The signal therefore shows IA from S_1 to S_2 and is not contaminated by the induced absorption from S_2, which appears at around 10000 cm^{-1} (Zhang et al, 2001) (this was checked by observing the monotonic decay of the signal at the subsequent delay times). The spectrum in cyclohexane was normalized to the 0–0 peak, while in toluene the 0–1 peak was chosen because of smoothness and strength similar to 0–0. The fitting results are shown by black smooth lines and the fit parameters are given in Table 1; Lorentzian line-shapes produced a fit of high quality. Interestingly, the fitting of NIR spectra shows a much better agreement with

the experiment than the absorption spectra, even though the 0–0 peaks are noisy due to their position at the limit of the detection spectral window. The high fidelity of the fit can be attributed to the lack of influence of ground state conformers at 500 nm excitation. The determined energy gaps ω_{12} imply that the S_1 state is positioned at 13760 and 13280 cm^{-1} in cyclohexane and toluene, respectively.

TA spectra in the visible

TA spectra of β-carotene in the visible were recorded both in cyclohexane and toluene. However, as the results in both solvents are qualitatively identical, only results in cyclohexane are considered further for the sake of clarity. Model calculations were done to fit the entire experimental data set. To assess the quality of the fit, the TA spectra are shown in Fig. 3 (experimental data shown in fuzzy lines, model data shown in smooth lines). Four representative spectra were selected at short (200 and 500 fs) and long (1 and 3 ps) delay times.

The parameters of the model can be summarized in two groups: "static parameters" that describe the line-shapes and "dynamic parameters" governing the population dynamics. The static parameters taken from the linear absorption fitting were used to calculate SE and GSB components of TA spectra. For the SE component, a Stokes shift of $\delta\omega_{\mathrm{St.}} = 400\,\mathrm{cm}^{-1}$ was used as determined from early delay time TA spectra. The line-shape parameters for the $S_1 \rightarrow S_\mathrm{n}$ transition were obtained by fitting the TA peak at $\sim 18000\,\mathrm{cm}^{-1}$ at long times, i.e., after the vibrational relaxation on S_1. A transition dipole moment ratio $\mu_{02}/\mu_{1n} = 1.17$ was found. The dynamic parameters that enter the population transfer rates are the energy gap ω_{12} and displacements d_1^{12}, d_2^{12}, and also the parameters of the bath (Balevičius Jr. et al, 2015). The former three values are taken from the NIR data (Table 1). The bath is modeled as an overdamped Brownian oscillator (May and Kühn, 2004; Valkunas et al, 2013), which is parametrized by the relaxation time $\tau = 163\,\mathrm{fs}$ and the reorganization energies for both internal conversion, $\lambda_\mathrm{ic} = 1200\,\mathrm{cm}^{-1}$, and vibrational relaxation, $\lambda_\mathrm{vr} = 150\,\mathrm{cm}^{-1}$. While λ_ic together with the corresponding FC factors governs the population transfer rates *between* the vibronic sub-levels on S_2 and S_1, λ_vr determines the vibrational relaxations *within* S_2 and S_1. The relaxation of the S_1 state is treated by phenomenologically including its exponential decay with a lifetime of 8.3 ps. The duration of the pump pulse was set to be $\tau_\mathrm{p} = 70\,\mathrm{fs}$, in agreement with the experimental value. The parameters are summarized in Table 1.

The spectral evolution in Fig. 3 is typical to carotenoids in solution (Polívka and Sundström, 2004). On the scale of hundreds of femtoseconds, an IA signal at ~18000 cm^{-1} is forming, which represents the $S_1 \rightarrow S_\mathrm{n}$ transition. This

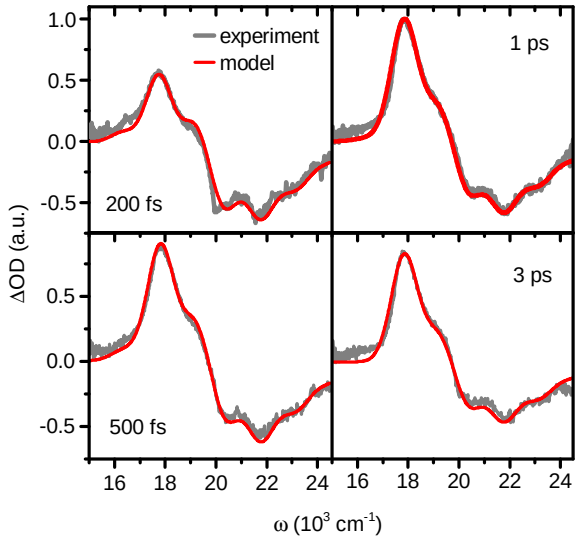

Fig. 3 TA spectra of β-carotene in cyclohexane after 500 nm excitation. Experimental data are shown as fuzzy lines, model calculations are represented by smooth lines

signal reaches its maximum at 1 ps and subsequently monoexponentially decays together with the GSB component (20000 cm^{-1} and above). There are several important details in this general picture. Firstly, at early times the signal is broader and slightly red-shifted with respect to the signal at 1 ps. The narrowing and blue-shifting of the IA is well known and is attributed to vibrational cooling within S_1 state (Andersson and Gillbro, 1995). The narrowing of the signal in the calculations arises directly from the model, while the blue-shift of the central frequency of IA was added phenomenologically shifting ω_{1n} by 200 cm^{-1} in 300 fs. This time-dependent Stokes shift is associated with all the unaccounted vibrational modes of the molecule, i.e., other than the two stretching modes which have been treated explicitly. Secondly, the shoulder at ~19500 cm^{-1} has been widely debated in the literature under the name of the so-called S^* state (Polívka and Sundström, 2009; Balevičius Jr. et al, 2016). In the current study this signal decays with the same lifetime as the main peak of IA at 17850 cm^{-1} and does not have to be treated as an electronic state additional to S_1 (Niedzwiedzki et al, 2016).

Dependence of the TA spectra on excitation wavelength

By fitting the TA spectra for 500 nm excitation we have determined all the model parameters. To study pump wavelength dependencies, we calculate TA spectra for different excitation wavelengths changing just the frequency of the pump pulse, ω_p, in the pumping term of Eq. 6. The model

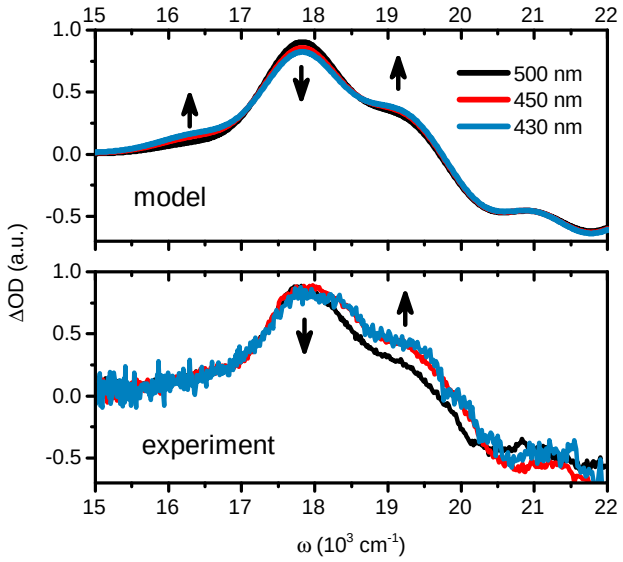

Fig. 4 TA spectra of β-carotene in cyclohexane at 500 fs delay for three excitation wavelengths. Top panel shows model calculations, bottom panel shows the experimental results. The arrows indicate the trends (starting from 500 nm excitation) at specific spectral regions associated with different vibronic transitions

results at 500 fs delay are shown in the top panel of Fig. 4; experimental results are shown in the bottom panel.

The arrows in Fig. 4 demonstrate the main trends when changing pump wavelength between 500 and 430 nm. The model calculations predict a decrease of the central peak of IA and simultaneous increase of the wings. However, these differences in the line-shapes gradually disappear in time. The IA spectrum has the same converged line-shape at 1 ps, regardless of the excitation frequency. The experimental results at 0.5 ps show a notable increase of the blue wing of IA, a slight decrease of the main peak and virtually no change in the red side. We attribute the latter lack of pump wavelength dependence to the fact that the signal is considerably noisier around 16000 cm^{-1} and below. Moreover, the signal-to-noise level is lower for shorter wavelength excitations due to the decreasing power of the pump pulse.

Discussion

From an experimental point of view, the excess excitation of carotenoids is achieved by tuning the excitation wavelength to a specific vibronic peak (Fig. 1), leading to the excitation naming: 0–0, 0–1 or 0–n excitation (Kosumi et al, 2005). In the context of VERA the precise vibrational levels covered by the excitation pulse become important for an adequate description of ensuing dynamics. The visually apparent vibronic peaks in the absorption spectrum do not belong to a single vibrational mode; they are largely a result of the vibronic progression from two symmetric carbon–carbon double- and single-bond (C=C and C–C) stretching modes (conf., stick spectrum in Fig. 1). Bearing in mind this internal multi-band structure of the absorption spectrum, one can specify which vibrational levels are being excited by a given pulse.

In order to analyze and rationalize the effects of tunable excitation of carotenoids in both earlier reports and the current study, we extend VERA by an exact treatment of initial populations after excitation (Eqs. 7 and 8). We primarily consider shorter wavelength excitations of carotenoids which populate higher-lying vibronic levels of S_2. Additionally we use the experimental NIR TA data to minimize the number of the free parameters. Our findings can be analyzed most efficiently by grouping them into two interdependent yet distinct sets of results. Firstly, we discuss the change of the TA line-shape upon excess excitation. Secondly, we analyze the effect of tunable excitation on the lifetime of the S_2 state, and re-evaluate results from TA and fluorescence excitation studies, with respect to our new findings on the curve displacement of the $S_2 \rightarrow S_1$ internal conversion.

Effects of vibrational cooling in the formation of the IA line-shape.

The broad line-shape of IA at early times in Fig. 3 represents the absorption from higher vibrational levels on S_1. This early, broad and slightly red-shifted IA signal with the lifetime of ~0.5 ps is sometimes attributed to an abstract "hot S_1" state (Andersson and Gillbro, 1995; Polívka and Sundström, 2004). Its formation along with subsequent transition to IA from the relaxed S_1 state is attributed to vibrational cooling. It has been proposed that vibrational cooling on the S_1 state is mediated by low-frequency vibrational modes (Billsten et al, 2002; de Weerd et al, 2002). However, our current and earlier modeling in (Balevičius Jr. et al, 2015) gives an alternative explanation. The apparent broadening of the IA signal at early times is a result of the initial absorption from higher-lying vibronic levels, $|S_1\rangle|a>0\rangle_1|b>0\rangle_2$. The later narrowing is due to relaxation to the vibrational thermalized state on S_1: $|S_1\rangle|0\rangle_1|0\rangle_2$. In the displaced harmonic oscillator model the transitions from vibronic levels $|S_1\rangle|a\rangle_1|b\rangle_2$ to vibronic levels $|S_n\rangle|a\pm1\rangle_1|b\pm1\rangle_2$ can have higher oscillator strength than the transitions to the levels $|S_n\rangle|a\rangle_1|b\rangle_2$, depending on the involved FC factors. Thus the sidebands around the central frequency ω_{1n} become larger upon increased displacements d_1^{1n}, d_2^{1n}.

This mechanism can readily be observed in Fig. 4. Upon the excitation of higher vibronic levels on S_2, the higher vibronic levels on S_1 become more populated at early times. Transitions $|S_1\rangle|a\rangle_1|b\rangle_2 \rightarrow |S_n\rangle|a-1\rangle_1|b\rangle_2, |S_n\rangle|a\rangle_1|b-1\rangle_2$ increase the signal at ~16500 cm^{-1}, while the transitions $|S_1\rangle|a\rangle_1|b\rangle_2 \rightarrow |S_n\rangle|a+1\rangle_1|b\rangle_2, |S_n\rangle|a\rangle_1|b+1\rangle_2$ increase the signal at ~19500 cm^{-1}. At the expense of these growths, the

signal at the central frequency is reduced. Although the measurement in Figure 4 doesn't show the increase of the red side of IA upon excess excitation, this is possibly the result of an increase in noise in this spectral range. However, earlier results in the literature clearly confirm this effect, conf., (Kosumi et al, 2005; Jailaubekov et al, 2011). The signal on the blue side of the central peak of IA, referred to as the S^* signal, has been previously discussed (Polívka and Sundström, 2009). It should be treated as the vibronic satellite of the main IA signal if it has the same lifetime as S_1 (Balevičius Jr. et al, 2015), while the difference in lifetime can be accounted for by introducing vibrationally hot ground state levels (Balevičius Jr. et al, 2016). In the current study the former treatment is applicable.

The increased line-width of the IA signal upon 450 nm and higher excitation has been suggested to be a result of increased conformational disorder, contributing to the signal generated by excess excitation (Billsten et al, 2005; Staleva et al, 2015). In our model this broadening appears without any additional assumptions, and it is rather a feature of the same mechanism describing vibrational cooling. Namely, the excess energy after internal conversion populates higher-lying vibrational levels more abundantly and increases the weight of their contribution in the total IA signal. The inhomogeneous line-broadening due to conformational disorder is encoded in the width parameter $\Delta\omega_{1n}$, conf., Eq. 2, which is not changed in our modeling.

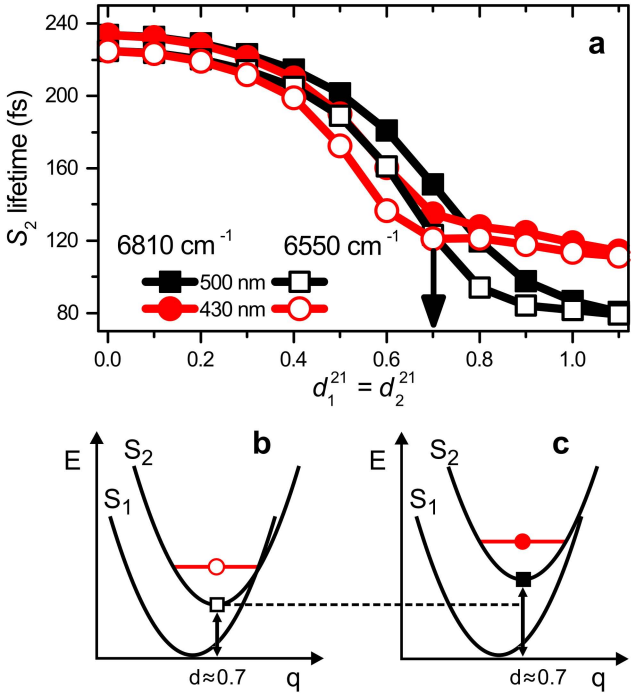

Fig. 5 Dependence of the S_2 state lifetime on the dimensionless displacements d_1^{12} and d_2^{12}. (a) The lifetimes are given for two energy gaps between the states S_1 and S_2 (6810 and 6550 cm^{-1} represented by full and empty symbols, accordingly), for excitations by 500 (squares) and 430 nm (circles) pulses. The arrow indicates a critical value beyond which the the lifetime upon excess excitation is increased for the 6550 cm^{-1} gap case. (b) and (c) Schematic representation of potential energy curves for smaller and larger energy gaps, accordingly, maintaining identical curve displacement. In (b) optimal transfer is achieved due to crossing of the curves. The energy shift in (c), emphasized by the dashed line, brings the curves away from each other and increases S_2 lifetime

Lifetime of the S_2 state.

The excitation pulses shown in Fig. 1 were kept spectrally narrow to selectively excite specific vibronic bands and to avoid the formation of ground state wavepackets (Christensson et al, 2009), which potentially hamper the analysis of relaxation dynamics. As a side effect of such narrow band excitation, we are unable to accurately measure the lifetime of the S_2 state. Despite such shortcomings, VERA in conjunction with the NIR TA data allows us to address the question of the S_2 lifetime from several perspectives. One possibility is to look directly at the evolution of the populations of $|S_2\rangle|a\rangle_1|b\rangle_2$ vibronic levels. Due to the fact that individual levels cannot be resolved in the TA experiment, we rather look at the total population of the S_2 state as the sum of its components, $n_2(t) = \sum_{ab} n_2^{ab}(t)$. The population evolution is interesting in that we can study the interplay between vibrational relaxation and internal conversion from S_2 to S_1. The rate of the internal conversion $S_2 \rightarrow S_1$ in our model is mainly governed by two parameters (Balevičius Jr. et al, 2015): the reorganization energy, λ_{ic}, and the displacements d_1^{12}, d_2^{12}. While the former parameter sets an overall amplitude of the rate and is insensitive to the specific vibrational levels from/to which the internal conversion takes place, the FC factors (governed by the displacements) make the process dependent on the specific levels involved. Therefore we have investigated the lifetime of the total population of S_2 as a function of the displacements. The lifetime is then evaluated by fitting the $n_2(t)$ evolution with a single-exponential decay.

The following analysis is general and not limited to β-carotene in a specific solvent. For the sake of simplicity we calculated the lifetime for identical values of both displacements $d = d_1^{12} = d_2^{12}$, a condition that well approximates the values of d parameters summarized in Table 1. In addition to that, we calculate the dependencies for two values of the energy gap ω_{12}. To keep this parameter realistic, we chose the larger and the smaller gaps to be 6810 and 6550 cm^{-1}, which corresponds to (but is not limited to) the retrieved values for cyclohexane and toluene, respectively (see Table 1). Without loss of generality, the reorganization energies are taken from the fit of the TA measurement in cyclohexane.

Fig. 5a shows the results of the calculation for two excitation wavelengths 500 (squares) and 430 nm (circles) and the two electronic energy gaps ω_{12}, 6810 and 6550 cm^{-1}

(full vs empty symbols). The first and most significant trend in Fig. 5a is the decrease in S_2 lifetime with increasing the displacements. Secondly, the decay is faster for smaller energy gap. And lastly, but most importantly for the current study, there is a region at $d \gtrsim 0.7-0.8$, in which S_2 lives for a shorter time when the lowest vibrational level is excited.

To rationalize these observations we turn to the semi-classical parabolic potential surface model, inspired by Marcus theory of electron transfer. In Figs. 5b and c the potential curves along one coordinate q are shown for the states S_1 and S_2. Fig. 5b is a schematic representation of the smaller energy gap ω_{12} configuration, while Fig. 5c depicts the situation for a larger energy gap, keeping the same displacement d of the upper curve. In such a semi-classical picture the optimal and fastest energy transfer takes place at the intersection points of the two parabolas.

Firstly, we elucidate why the smaller energy gap yields faster decay at identical displacements. Fig. 5b demonstrates the crossing of the two potential curves at a certain excited vibronic level, in the configuration of the inverted Marcus regime. Such configuration results in the optimal transfer from a vibrationally hot excited state. In the case of larger energy gap (Fig. 5c) the two curves are not yet in contact and a larger displacement is needed to maximize the transfer rate. This explains why the empty symbols represent shorter lifetimes than the full symbols at all displacements in Fig. 5a.

Next, we explain why optimal transfer from the lowest vibrational level is achieved at larger displacements (regardless of the energy gap). As can be seen from the schematic representations for the lowest excitations (shown by squares), the bottom of the upper parabola will always cross the lower parabola at larger displacements than any other point of the upper parabola. The shortest lifetime values are obtained for excitations into the lowest vibrational states at displacements larger than 1 — the maximal overlap of vibronic states is achieved there. At these displacement values higher vibronic levels are detuned from the optimal overlap, hence excess excitation leads to slower relaxation of S_2 state. In principle, the displacements could be increased even further, yet the NIR results (either in this study or in other reports (Polívka et al, 2001)) indicate that such large displacements are unrealistic.

Finally, the presented analysis explains how two possible internal conversion regimes emerge: a region where the decay is faster upon excitation with excess energy ($d < 0.7$, the inverted Marcus regime) and a region where it is slower ($0.7 < d < 1.1$). Are these parameters realistic? The curves near the critical point $d \approx 0.7-0.8$ imply sensitivity of the S_2 lifetime trends to the chosen solvent. From inspection of Table 1 we see that the values of d_1^{12}, d_2^{12} are very near the critical point, some slightly above, some below. In fact, the calculations with the experimentally determined values suggest that the S_2 state of β-carotene should decay faster after excess excitation in cyclohexane (144 fs after 500 nm excitation vs 132 fs after 430 nm excitation) and slower in toluene (106 fs vs 121 fs, respectively). The actual numbers should be taken with caution because of the invoked Markov approximation and the fact that the bath relaxation time is of the same order as the obtained lifetimes, but the general trend should hold. Literature confirms this ambiguous prediction: a slowdown of S_2 relaxation upon excess excitation has been reported for β-carotene and lycopene in benzene and *n*-hexane (Kosumi et al, 2005). Slowdown was also found for synthetic carotenoid–phthalocyanine dyads in toluene (Kloz et al, 2012). The opposite trend was reported for neurasporene in *n*-hexane (Zuo et al, 2007) and zeaxanthin in methanol (Billsten et al, 2005), although later measurements of zeaxanthin homologues in tetrahydrofuran showed no change at all (Staleva et al, 2015). This indicates the need to systematically apply the methodology presented in this work to several carotenoids in a number of solvents. The essential prerequisites for such a study are TA experiments with NIR probing, covering the S_1–S_2 IA band, and a sufficiently short instrumental response function for TA in the visible, to resolve the S_2 lifetime.

There is, however, an indirect way of testing the presented theory experimentally, without the need to invoke TA studies with demanding time resolutions. The change of S_2

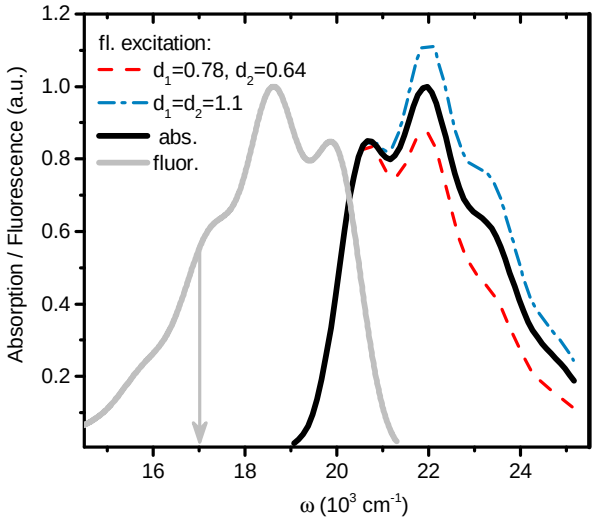

Fig. 6 Calculated absorption, fluorescence and fluorescence excitation spectra of β-carotene in cyclohexane. Absorption (black line) corresponds to the dashed line in Fig. 1, fluorescence (gray line) is calculated using the same parameters plus the Stokes shift of 400 cm^{-1}. The gray arrow indicates the wavenumber, 17000 cm^{-1}, at which the emission signal for the fluorescence excitation spectrum was integrated (see text for details). The fluorescence excitation spectrum was calculated for the parameters of β-carotene in cyclohexane (dashed line) and additionally for displacement values changed to $d_1^{12} = d_2^{12} = 1.1$ (dash-dotted line)

lifetime upon excess excitation should manifest itself in fluorescence excitation spectra. In this simple linear method, the fluorescence of the sample at a given detection wavelength is recorded as a function of the wavelength of a tunable narrow-band excitation source. For β-carotene, a decrease of signal intensity in the blue as compared to the linear absorption spectrum is well documented (DeCoster et al, 1992; Dilbeck et al, 2016). We demonstrate qualitatively how this result is explained by our theory via the following procedure. First, we create the initial condition to represent a narrow-band pump pulse used in the fluorescence excitation spectroscopy. The pumping term in Eq. 6 is replaced by

$$p_{ab}(t,\omega) = \Gamma(t,\tau_{\mathrm{p}}) f_{02}(0,0,a,b)\times,$$
$$[\sigma(\omega - 0.5\Delta\omega_{\mathrm{p}} - \omega_{02} - \omega_{0,0,a,b}, \Delta\omega_{02}) +$$
$$\sigma(\omega + 0.5\Delta\omega_{\mathrm{p}} - \omega_{02} - \omega_{0,0,a,b}, \Delta\omega_{02})],$$

which approximates the pump pulse as a square pulse of width $\Delta\omega_{\mathrm{p}}$=100 cm^{-1}. Then the SE signal, defined in Eq. 4, is integrated over in time at ω_{fl}=17000 cm^{-1}. This integral is a function of excitation wavelength and defines the emissive capability of the molecule, hence, we denote it by an auxiliary function:

$$\varphi(\omega) = \frac{1}{N}\int_0^\infty \mathrm{d}t |E(\omega_{\mathrm{fl}},t)|_{\omega_{\mathrm{p}}=\omega}, \tag{8}$$

where $N = \int_0^\infty \mathrm{d}t |E(\omega_{\mathrm{fl}},t)|_{\omega_{\mathrm{p}}=\omega_{02}}$ is the norm such that $\varphi(\omega \leq \omega_{02}) = 1$ or in other words the emission after 0–0 excitation is set to unity. Since the signal strength in the fluorescence excitation is a combination of two factors — the emissive capability at ω_{fl} and the absorbance at the specific excitation wavelength — we represent it as the product of the function $\varphi(\omega)$ and the absorption spectrum:

$$F(\omega) = \varphi(\omega) I_0^{00}(\omega). \tag{9}$$

The calculated fluorescence excitation spectrum of β-carotene together with the absorption and fluorescence spectra are shown in Fig. 6. The gray arrow indicates the wavelength at which the emission is calculated. The fluorescence excitation spectra are calculated for the parameters of β-carotene in cyclohexane (dashed line) and for the same parameters except the displacements d_1^{12}, d_2^{12} which are set to 1.1 (dash-dotted line). As can be seen, the actual β-carotene parameters yield the fluorescence excitation spectrum qualitatively similar to the one reported in (DeCoster et al, 1992). The decrease of signal strength at higher frequencies reflects the reduction of S_2 lifetime after the excitation into higher-lying vibronic levels. An efficient relaxation channel diverts the energy towards S_1 hence preventing fluorescence. An opposite and counter-intuitive situation is observed for the larger displacement values of 1.1: the more efficient energy transfer occurs from the lowest-lying vibronic level, hence more fluorescence is detected when the higher-lying levels are excited. This effect could explain the fluorescence excitation spectra reported for spheroidene and neurasporene (Fujii et al, 1998), where the authors suggested that the increase of the fluorescence excitation signal in the blue was due to impurities.

Conclusions

In this study we have demonstrated how the rigorous treatment of high-frequency vibrational stretching modes in carotenoids explains the dependence of TA spectra on the wavelength of the pump pulse for β-carotene in solution. We have shown that the increased line-width of the induced absorption after excitations into higher vibrational levels of S_2 results from vibrational cooling via the aforementioned high-frequency modes, which means that neither low-frequency modes nor structural inhomogeneities need to be invoked. Furthermore, we have demonstrated how the effects of excess excitation on the lifetime of the S_2 state critically depend on the caro-tenoid–solvent interaction, which can be quantified by the curve displacements between the potential energy surfaces. The presented theory explains why both a speed-up and a slow-down of the internal conversion from S_2 to S_1 upon excess excitation can be observed, depending on energy gap between S_2 and S_1 and on curve displacements. Finally, we suggest that a systematic study following the presented methodology should be carried out both experimentally and theoretically on sets of carotenoids in various solvents to confirm (or deny) the presented findings on S_2 lifetime.

Acknowledgements V. B. acknowledges funding by the Leverhulme Trust Research Project Grant RPG-2015-337. J. H. and C. N. L. acknowledge funding by the Austrian Science Fund (FWF): START project Y 631-N27. D. A. acknowledges support by the Research Council of Lithuania (No: MIP-090/2015). G. C. acknowledges support by the European Research Council Advanced Grant STRATUS (ERC-2011-AdG No. 291198) . G. C. and J. H. acknowledge funding by Laserlab-Europe (EU-H2020 654148).

References

Andersson PO, Gillbro T (1995) Photophysics and dynamcis of the lowest excited singlet-state in long susbtituted polyenes with implications to the very long-chain limit. J Chem Phys 103(7):2509–2519

Balevičius Jr V, Galestian Pour A, Savolainen J, Lincoln CN, Lukeš V, Riedle E, Valkunas L, Abramavicius D,

Hauer J (2015) Vibronic energy relaxation approach highlighting deactivation pathways in carotenoids. Phys Chem Chem Phys 17:19,491–19,499

Balevičius Jr V, Abramavicius D, Polívka T, Galestian Pour A, Hauer J (2016) A unified picture of S* in carotenoids. J Phys Chem Lett 7:3347–3352

Billsten HH, Zigmantas D, Sundström V, Polívka T (2002) Dynamics of vibrational relaxation in the S_1 state of carotenoids having 11 conjugated C=C bonds. Chem Phys Lett 355:465–470

Billsten HH, Pan J, Sinha S, Pascher T, Sundström V, Polívka T (2005) Excited-state processes in the carotenoid zeaxanthin after excess energy excitation. J Phys Chem A 109:6852–6859

Cerullo G, Silvestri SD (2003) Ultrafast optical parametric amplifiers. Review of Scientific Instruments 74(1):1–18

Chábera P, Fuciman M, Hřibek P, Polívka T (2009) Effect of carotenoid structure on excited-state dynamics of carbonyl carotenoids. Phys Chem Chem Phys 11(39):8795–8803

Christensson N, Milota F, Nemeth A, Sperling J, Kauffmann HF, Pullerits T, Hauer J (2009) Two-dimensional electronic spectroscopy of β-carotene. J Phys Chem B 113(51):16,409–16,419

Christensson N, Milota F, Nemeth A, Pugliesi I, Riedle E, Sperling J, Pullerits To, Kauffmann HF, Hauer J (2010) Electronic double-quantum coherences and their impact on ultrafast spectroscopy: The example of β-carotene. J Phys Chem Lett 1:3366–3370

DeCoster B, Christensen RL, Gebhard R, Lugtenburg J, Farhoosh R, Frank HA (1992) Low-lying electronic states of carotenoids. Biochimica et Biophysica Acta (BBA) - Bioenergetics 1102(1):107 – 114

Dilbeck PL, Tang Q, Mothersole DJ, Martin EC, Hunter NC, Bocian DF, Holten D, Niedzwiedzki DM (2016) Quenching capabilities of long-chain carotenoids in light-harvesting-2 complexes from Rhodobacter sphaeroides with an engineered carotenoid synthesis pathway. J Phys Chem B 120:5429–5443

Dobryakov AL, Kovalenko SA, Ernsting NP (2005) Coherent and sequential contributions to femtosecond transient absorption spectra of a rhodamine dye in solution. J Chem Phys 123(4):44,502

Frank H, Young A, Britton G, Cogdell R (eds) (1999) The Photochemistry of Carotenoids, Advances in Photosynthesis and Respiration, vol 8. Springer Netherlands

Frank HA, Cogdell RJ (1996) Carotenoids in photosynthesis. Photochem Photobiol 63(3):257–264

Fujii R, Onaka K, Kuki M, Koyama Y Yand Watanabe (1998) The $2A_g^-$ energies of all-trans-neurosporene and spheroidene as determined by fluorescence spectroscopy. Chem Phys Lett 288:847–853

Hauer J, Maiuri M, Viola D, Lukes V, Henry S, Carey AM, Cogdell RJ, Cerullo G, Polli D (2013) Explaining the temperature dependence of spirilloxanthin's S* signal by an inhomogeneous ground state model. J Phys Chem A 117:6303–6310

Jailaubekov AE, Vengris M, Song SH, Kusumoto T, Hashimoto H, Larsen DS (2011) Deconstructing the excited-state dynamics of β-carotene in solution. J Phys Chem A 115:3905–3916

Kloz M, Pillai S, Kodis G, Gust D, Moore TA, Moore AL, van Grondelle R, Kennis JTM (2012) New light-harvesting roles of hot and forbidden carotenoid states in artificial photosynthetic constructs. Chem Sci 3:2052–2061

Kosumi D, Yanagi K, Nishio T, Hashimoto H, Yoshizawa M (2005) Excitation energy dependence of excited states dynamics in all-*trans*-carotenes determined by femtosecond absorption and fluorescence spectroscopy. Chem Phys Lett 408:89–95

Larsen DS, Papagiannakis E, Stokkum IHM, Vengris M, Kennis JTM, van Grondelle R (2003) Excited state dynamics of β-carotene explored with dispersed multi-pulse transient absorption. Chem Phys Lett 381:733–742

Lukeš V, Christensson N, Milota F, Kauffmann HF, Hauer J (2011) Electronic ground state conformers of β-carotene and their role in ultrafast spectroscopy. Chem Phys Lett 506(1–3):122–127

May V, Kühn O (2004) Charge and Energy Transfer in Molecular Systems. Wiley-VCH Verlag GmbH, Weinheim

Nakamura R, Fujii R, Nagae H, Koyama Y, Kanematsu Y (2004) Vibrational relaxation in the $1B_u^+$ state of carotenoids as determined by Kerr-gate fluorescence spectroscopy. Chem Phys Lett 400:7–14

Nakamura R, Wang P, Fujii R, Koyama Y, Hashimoto H, Kanematsu Y (2006) Vibrational relaxation pathways in the electronic excited state of carotenoid. J Lumin 119–120:442–447

Niedzwiedzki DM, Hunter CN, Blankenship RE (2016) Evaluating the nature of so-called S*-state feature in transient absorption of carotenoids in light-harvesting complex 2 (LH2) from purple photosynthetic bacteria. J Phys Chem B 120(43):11,123–11,131

Papagiannakis E, van Stokkum IHM, Vengris M, Cogdell RJ, van Grondelle R, Larsen DS (2006) Excited-state dynamics of carotenoids in light-harvesting complexes. 1. exploring the relationship between the S1 and S* states. J Phys Chem B 110(11):5727–5736

Polívka T, Sundström V (2004) Ultrafast dynamics of carotenoid excited states – from solution to natural and artificial systems. Chem Rev 104:2021–2071

Polívka T, Sundström V (2009) Dark excited states of carotenoids: Consensus and controversy. Chem Phys Lett

477:1–11

Polívka T, Zigmantas D, Frank HA, Bautista JA, Herek JL, Koyama Y, Fujii R, Sundström V (2001) Near-infrared time-resolved study of the S_1 state dynamics of the carotenoid spheroidene. J Phys Chem B 105:1072–1080

Staleva H, Zeeshan M, Chábera P, Partali V, Sliwka HR, Polívka T (2015) Ultrafast dynamics of long homologues of carotenoid zeaxanthin. J Phys Chem A 119(46):11,304–11,312

Takaya T, Iwata K (2014) Relaxation mechanism of β-carotene from s_2 $(1b_u^+)$ state to s_1 $(2a_g^-)$ state: Femtosecond time-resolved near-IR absorption and stimulated resonance Raman studies in 900–1550 nm region. J Phys Chem A 118(23):4071–4078

Valkunas L, Abramavicius D, Mančal T (2013) Molecular Excitation Dynamics and Relaxation. Wiley-VCH, Weinheim

van Amerongen H, Valkunas L, van Grondelle R (2000) Photosynthetic Excitons. World Scientific, Singapore

de Weerd FL, van Stokkum IHM, van Grondelle R (2002) Subpicosecond dynamics in the excited state absorption of all-*trans*-β-carotene. Chem Phys Lett 354:38–43

Wendling M, Pullerits T, Przyjalgowski MA, Vulto SIE, Aartsma TJ, van Grondelle R, van Amerongen H (2000) Electron-vibrational coupling in the Fenna-Matthews-Olson complex of Prosthecochloris aestuarii determined by temperature-dependent absorption and fluorescence line-narrowing measurements. J Phys Chem B 104:5825–5831

Young AJ, Britton G (eds) (1993) Carotenoids in Photosynthesis. Chapman & Hall, London

Zhang JP, Skibsted LH, Fujii R, Koyama Y (2001) Transient absorption from the $1B_u^+$ state of all-*trans*-β-carotene newly identified in the near-infrared region. Photochem Photobiol 73(3):219–222

Zuo P, Sutresno A, Li C, Koyama Y, Nagae H (2007) Vibrational relaxation on the mixed vibronic levels of the $1B_u^+$ and $1B_u^-$ states in all-trans-neurosporene as revealed by subpicosecond time-resolved, stimulated emission and transient absorption spectroscopy. Chem Phys Lett 440:360–366